

# Minimal mechanism for fluidic flocks in interacting active colloids

Arvin Gopal Subramaniam,<sup>1,2,\*</sup> Sagarika Adhikary,<sup>1,2,†</sup> and Rajesh Singh<sup>1,2,‡</sup>

<sup>1</sup>*Department of Physics, Indian Institute of Technology Madras, Chennai, India*

<sup>2</sup>*Center for Soft and Biological Matter, IIT Madras, Chennai, India*

Collective motion as a flock is a widely observed phenomenon in active matter systems. Finding possible mechanisms of attaining a global polar order via dynamical mechanisms - without any explicit alignment interaction - is an area of active current research. Here, we report a flocking transition sustained purely by chemo-repulsive torques at low to medium densities in a system of chemically interacting colloidal particles. The basic requirements to sustain the flock are excluded volume repulsions and deterministic long-ranged net repulsive torques, with the time scale individual colloids move a unit length being dominant with respect to the time they deterministically sense chemicals. Switching on the translational repulsive forces renders the flock a crystalline structure. The generality of this phenomenon is displayed for a range of attractive translational forces to which the flock is robust. We rationalize these results with a phenomenological hydrodynamical model.

The collective swarming behaviour of interacting agents - also called flocking [1] - has been a topic of sustained interest in the field of non-equilibrium statistical physics. Flocking is also an ubiquitous phenomena in the natural world. Paradigmatic models that incorporate short-ranged alignment interactions to study flocking have been extensively studied [1–4] and continue to be investigated [5, 6]. In the Vicsek model [2], local alignment interactions among the individual agents can lead to transition from a disordered state to one with large-scale, coordinated movement. The flocking transition in Vicsek-like models with short-range interactions has been widely studied, and traveling density bands are observed at the onset of transition [3, 4, 7, 8].

The possibility of attaining an emergent global polar order (flocking) arising purely out of dynamical particle-based models is a subject of recent interest. Studies on these include those studying the interplay between non-equilibrium phase separation and other collective dynamics [9–12], those that study the effect of velocity alignment interactions [13–15], models incorporating attractive interactions [16, 17], history-dependence [18, 19], and those that exclusively study the effect of repulsive forces and torques [20, 21]. Though various possible mechanisms deviating from the Vicsek-like phenomenology have been established, the explicit relevance of the separate force and torque contributions have not been established. For instance, migrating cells that display a global polarity have been known to display chemotactic attractive interactions in addition to (among others) either a contact “inhibited” or “attracted” locomotion - akin to a long-ranged torque of either repulsive or attractive nature [17, 22, 23]. Thus, open questions remain on the minimal ingredients and mechanism at play arising separately from the rotational and translational components.

In this letter, we report a novel flocking mechanism for polar liquids where colliding pair particles have to sufficiently slowly rotate in response to chemical gradients before moving a unit distance. The basic ingredients that are *sufficient* to produce such a flock are thus (i) short-ranged excluded volume repulsion, and (ii) long-ranged (chemo) repulsive torques. There is no need for any additional (chemo)repulsive translational forces between the particles. The incorporation of long-ranged translational chemo-repulsive forces between the particles induces instead a crystalline flock (with regular lattice spacing). We first report our results from numerical simulations by mapping phase diagrams. The numerical simulations are rationalised via a phenomenological hydrodynamic model. In what follows, we describe our model and detail our results.

*Model of chemically interacting colloids:* We consider a set of  $N$  chemically interacting polar colloids, where chemical is assumed to be instantaneously deposited on the colloidal surfaces [24–27]. Hence, the interactions between the colloids do not contain a memory of previous trajectories and take a spatially long-ranged (as we show) gravitational-like  $\sim 1/r^2$  form. We model the  $i$ th active particle as a colloid particle centered at  $\mathbf{r}_i = (x_i, y_i)$ , confined to move in two-dimensions, which self-propels with a speed  $v_s$ , along the directions  $\mathbf{e}_i = (\cos \theta_i, \sin \theta_i)$ . Here  $i = 1, 2, 3, \dots, N$  and  $\theta_i$  is the angle made by the orientation  $\mathbf{e}_i$  with respect to the positive  $x$ -axis. The orientation  $\mathbf{e}_i$  of the  $i$ th particle, given in terms of the angle  $\theta_i$ , changes due to coupling its dynamics to the dynamics of a phoretic (scalar) field  $c$ , as we describe below. The position  $\mathbf{r}_i$  and orientation  $\mathbf{e}_i$  of the  $i$ th particle is updated as:

$$\frac{d\mathbf{r}_i}{dt} = \mathbf{V}_i, \quad \frac{d\mathbf{e}_i}{dt} = \boldsymbol{\Omega}_i \times \mathbf{e}_i. \quad (1)$$

Here, the translational velocity  $\mathbf{V}_i$  and angular velocity  $\boldsymbol{\Omega}_i$  of the  $i$ th particle are given as:

$$\mathbf{V}_i = v_s \mathbf{e}_i + \chi_t \mathbf{J}_i + \mu \mathbf{F}_i + \sqrt{2D_t} \boldsymbol{\eta}_i^T, \quad (2a)$$

$$\boldsymbol{\Omega}_i = \chi_r (\mathbf{e}_i \times \mathbf{J}_i) + \sqrt{2D_r} \boldsymbol{\eta}_i^R. \quad (2b)$$

\* Contributed equally; ph22d800@smail.iitm.ac.in

† Contributed equally; a.sagarika@physics.iitm.ac.in

‡ rsingh@physics.iitm.ac.in

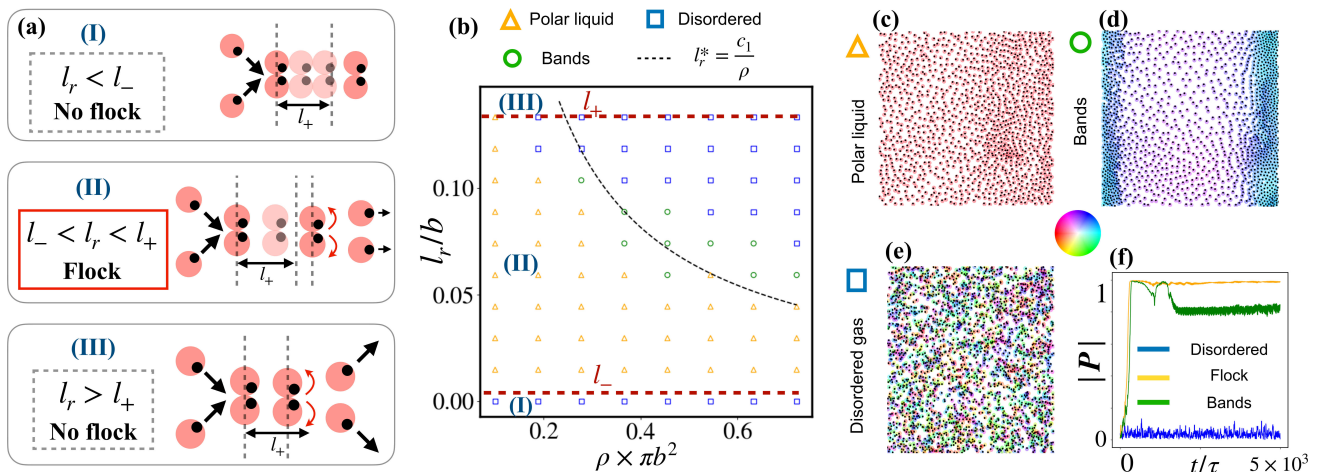


FIG. 1. Polar liquid flock for  $\chi_t = 0$ . (a) Schematic of the mechanism for formation of fluidic flocks. *Top-to-bottom*: Series of scenarios depicted corresponding to parameters choices labelled in (b).  $l_+$  and  $l_-$  are annotated in dashed red in (b), with the density dependent  $l_+$  in dashed black. The middle panel (II) shows the pair collision mechanism that would produce a flock; this occurs if the chemical sensing occurs after sliding a length  $l_+$ . Top (I) and bottom (III) panels show scenarios where the chemical response is either too slow or too quick, such that a stable flock cannot be formed. (b) Phase diagram in the  $(\rho, l_r/b)$  plane. Symbols here and throughout the paper denoting a flock (yellow triangle), disordered gas (blue squares), and bands (green circles). Snapshots of the respective phases are shown in (c)-(e) respectively (color coding for orientation of each particle is in middle panel). (f) The evolution of the polarization is displayed for the corresponding states (similarly colored).

For full generality, Eq. (2) is written with both translational and rotational terms, the respective chemical susceptibilities are denoted  $\chi_t$  and  $\chi_r$  respectively. Additionally,  $\mu$  is mobility,  $D_t$  and  $D_r$ , are respectively, translational and rotational diffusion constants of the particle, while  $\eta_i^T$  and  $\eta_i^R$  are white noises with zero mean and no correlation in time. The inter-particle interaction (of chemical origin) is given in terms of the phoretic current  $\mathbf{J}_i$ , as we explain below. The term proportional to  $\chi_r$  in Eq.(2) drives orientational changes (turning away from each other if  $\chi_r > 0$ ) through interparticle chemical interactions. Similarly, the term proportional to  $\chi_t$  ensures repulsion in the positional dynamics if  $\chi_t > 0$ . Here, both  $\chi_r$  and  $\chi_t$  are positive (unless otherwise stated) and the system is said to be *chemo-repulsive*.

To preclude overlap of the particles, there is a body force on the particles:  $\mathbf{F}_i = -\nabla_i \mathcal{U}$ , where  $\mathcal{U}$  is given by  $\mathcal{U} = \sum_{i < j} \mathcal{U}^e(\mathbf{r}_i, \mathbf{r}_j)$ . Here  $\mathcal{U}^e$  is a repulsive potential avoiding overlap of particles. With  $b$  as the colloidal radius, we choose  $\mathcal{U}^e$  to be of the form:  $\mathcal{U}^e = k^e (r_{ij} - 2b)^2$  if  $r_{ij} < 2b$ , while it vanishes otherwise. Here  $r_{ij} = |\mathbf{r}_{ij}|$ , with  $\mathbf{r}_{ij} = \mathbf{r}_i - \mathbf{r}_j$ , while  $k^e$  is a constant, which determines the strength of the repulsive force, which precludes overlap of particles.

The phoretic interactions between the particles is given in terms of  $\mathbf{J}_i$  (see Eq. (2)), which is defined as:  $\mathbf{J}_i(t) = -[\nabla c(\mathbf{r}, t)]_{\mathbf{r}=\mathbf{r}_i}$ , where  $c(\mathbf{r}, t)$  is the concentration of the chemicals that mediate the interaction (e.g filled micelles in an oil-emulsion system [18, 28]). For instantaneous deposition on the surface, the equation to be solved is  $D_c \nabla^2 c(\mathbf{r}, t) + \sum_{i=1}^N c_0 \delta(\mathbf{r} - \mathbf{r}_i) = 0$ , where  $D_c$  is the diffusion coefficient of the filled micelles and

$c_0$  is emission constant of the micelles. The solution is:  $\mathbf{J}_i = \mathcal{D} \sum_j \mathbf{r}_{ij} / r_{ij}^3$ , where  $\mathcal{D} = c_0 / D_c$ . This form of the current is used in Eq.(2) to run dynamical simulations.

The position and orientations of the particles are updated using a forward Euler-Maruyama method (equation 1). Initially particles are distributed randomly over the two-dimensional space. The initial orientations are also randomly distributed over the range of angles  $[-\pi, +\pi]$  (angles are computed with respect to the positive  $x$ -axis). Periodic boundary conditions are applied on both the  $x$ -axis and  $y$ -axis. To compute chemical interactions using the expression of  $\mathbf{J}_i$ , we need to sum over periodic images. We have used a regular summation convention for all results reported here, and checked these with the Ewald summation convention for selected parameter values [29]. Detailed set of parameters to generate each figures is given in the SI.

*Main results*: We first summarize our main results. The main schematic of the mechanism that we report is presented in Fig. 1(a). In particular, we report here polar fluids that are obtained without translational repulsion (Fig. 1(a) - *middle* panel). These flocks are obtained only if pair colloids move at least a distance  $l_+$  before deterministically rotating due to sensing of chemical gradients. Switching on the  $\chi_t$  we obtain crystalline flocks that are obtained via a combination of repulsive torques and forces (Fig. 2(b)); we also find these crystals for (a narrow range of) *attractive* forces (Fig. 3(a)). For the rest of the paper we denote the former as ‘‘Chemorepulsive Liquid Flocks’’ (CLF), and the later as ‘‘Chemorepulsive Crystalline Flocks’’ (CCF).

*CLFs via long-ranged repulsive torques*: We first con-

sider the case of  $\chi_t = 0$ , thus repulsions are only short-ranged in the system via  $\mathbf{F}_i$ . The phase diagram delimiting polar flocks, bands, and disordered states are shown in Figure 1(b). The states are delimited via the mean global polarization of the system at the steady state,  $\langle |\mathbf{P}| \rangle_{ss}$ , where  $\mathbf{P} = \frac{1}{N} \sum_{i=1}^N \frac{\mathbf{e}_i}{|\mathbf{e}_i|}$ . On the  $(\rho, \chi_r)$  plane (Fig. 1(b)), we see that low density flocks are sustained, that are eventually destabilized at sufficiently high repulsion and densities [30]. These flocks have evidently a liquid-like spatial structure (Fig. 1(c); see also Fig. 2(c)) [20, 31, 32]. The density field  $\rho$  is thus not homogeneous across the system (see Fig. 1(b); (see also SI Section VI)). We note that  $\tau = b/v_s$  is the spontaneous propulsion time scale.

The phenomenology of the CLF can also be understood by a comparison of the relevant length (or equivalently time) scales of the problem. First, we write down natural length scales that arise out of the equations of motion (1)-(2). They are:

$$l_r = \frac{\chi_r b}{v_s}, \quad l_t = \frac{\chi_t}{bv_s}. \quad (3)$$

They are, respectively, the deterministic rotation and translational lengths; these quantify the length scales within the system where colloids instantaneously sense long-ranged chemical gradients for the rotational and translational dynamics respectively [33]. From the phase diagram, we see that there are separate length scales that arise as a consequence of the collective many-body dynamics. Let us denote  $l_-$  as the smallest length to sustain the CLF (corresponding to the lowest transition line),  $l_\rho$  as the (density dependent) length scale above which the CLF is not sustained - we will explicitly derive this from a phenomenological model.  $l_+$  is the largest length scale (independent of density) above which there is no CLF. From simulations, we find these values to be  $l_- \approx 0.01b$  and  $l_+ \approx 0.12b$ . The mechanism for the CLF can then be understood as a competition between  $l_r$  and  $\{l_-, l_+, l_\rho\}$ ; this is illustrated in Fig. 1(a) (annotated accordingly in the phase diagram of 1(b)). In the low density region (away from  $l_\rho$ ), we consider a series of transitions from disorder-to-order-to-disordered phases. For  $l_r < l_-$  (top), we have a *sub-deterministic* sensing of the chemicals; here the orientational changes of the colloids are too slow compared to the free movement time, hence local polar order cannot be sustained. Increasing  $l_r$ , in the regime of  $l_- < l_r < l_+$  (middle), we have that the chemical response time fast enough such that local polar order is sustained, but still sufficiently slow to break forward-backward symmetry at the pair collision level. Finally for  $l_r > l_+$ , the chemical response is sufficiently quick such that there is no symmetry breaking at the pair collision level. We conclude that, putatively, pair colloids have to *slide* at least a distance  $l_+$ , before deterministically turning away, as the underlying mechanism for the CLF. We note that other length scales that exist for the problem, for instance the colloidal diameter (within which excluded volume interactions take place)

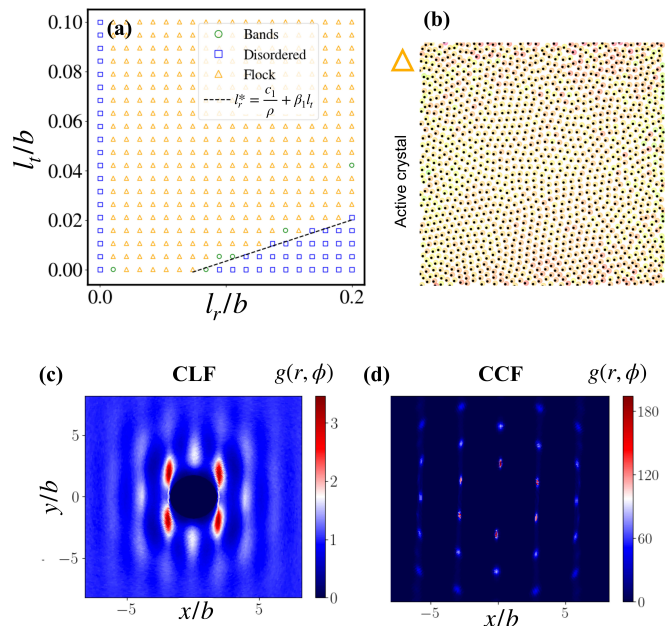


FIG. 2. (a) Phase diagram in the  $(l_r/b, l_t/b)$  plane for the case of  $\chi_t > 0$ . Dashed line refers to lower bound on  $\chi_r$ , solid line for lower bound on  $\chi_r$  from (5). (b) Shows a snapshot of the CCF phase (same color scheme as in Fig (1)). (c) and (d) compare  $g(r, \phi)$  for the case of the CLF and the CCF.

$d = 2b$ , the mean free path length  $\frac{1}{\sqrt{\rho}}$ , etc., but they are substantially larger than the upper bound of  $l_+$  reported here. For larger  $\rho$ , the upper length limit is  $l_\rho$  - this density dependence we will show later arises from a minimal hydrodynamic model.

*Effect of long-ranged translational repulsion:* We now switch on  $\chi_t$  and ask how the properties of the flock differ. On the  $(\chi_r, \chi_t)$  plane, we find that there is a clear region of flocking for non-zero  $\chi_t$  (see Figure 2(a)). We further find that the flocks have crystalline order (see Figure 2(b),(d)). Such crystalline flocks in repulsive systems have been recently reported [21]. Similarly to the CLF, the CCF destabilized by sufficiently high rotational torques. In effect, we see an additional length scale  $l_r^*(\rho, l_t)$  which  $l_r$  cannot exceed. We will see below that to a first approximation,  $l_r$  is linear in  $l_t$  with dependencies on both  $v_s$  and  $\rho$ . Thus, crystalline flocks require colloids to positionally align via translational repulsion (independent of excluded volume interactions) quicker than they deterministically rotate. We note that if this repulsion is too strong, the CCF is destabilized to a disordered gas (not shown here).

The difference in spatial structure between the CLF and CCF is readily distinguished by the pair correlation function  $g(r) = \frac{1}{N} \sum_{i,j} \delta(r - |\mathbf{r}_i - \mathbf{r}_j|)$ . This is shown in SI Section II, where we clearly see the respective solid and liquid-like signatures [20]. A closely related quantity [34] is the polar pair correlation  $g(r, \phi)$  which explicitly depends on the orientations of the colloids. Here,  $\cos(\phi_{ij}) = \mathbf{e}_i \cdot (\hat{\mathbf{r}}_i - \hat{\mathbf{r}}_j)$ [34]. For the CLF, we



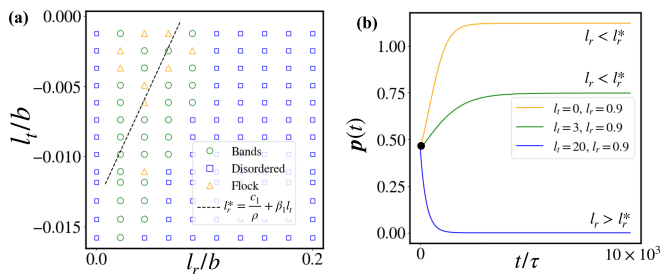


FIG. 3. (a) Phase diagram in the  $(\chi_r, \chi_t)$  plane for the case of  $\chi_t < 0$  for the particle-based model. The transition line is extrapolated from (2)(a). (b) Plot of  $p(t)$  using the simulation of continuum equations. Parameters used are  $\rho_0 = 0.8$ ,  $D_\rho = a_2 = 5$ ,  $u_0 = u_1 = v_s = 1$ , and  $a_1 = 0.2$ .

see that there are quadrants where neighbours are more likely to be found (2(c)), as opposed to the hexagonal lattice structure of the CCF (2(d)). In the case of CCF, the intensity (proportional to the probability of finding the particle from the reference - see SI Section II) in the well-localized hexagonal positions of the crystal are substantially higher than in the CLF, which are instead less intense with a greater relative spread. The quadrant-like distribution indicate the repulsive torque-induced turn away of the particles in the forward and backward direction of the reference particle. An additional feature of the CLF is that they have a steady-state persistent fluctuations of both density and polarization fields (dynamical steady-state - note that our simulations are noiseless), which is absent in the CCF (SI Section VI). Further, we note that both the CCF and CLF show an enhanced number fluctuations  $\langle (\Delta N)^2 \rangle \sim N^\alpha$  with  $\alpha \sim 1.7$ , a signature of hydrodynamic flocks [35, 36] (SI Section VI).

To further support the robustness of the mechanism we report CLFs arising repulsive torques with the addition of long-ranged *attractive* interactions, thus  $\chi_t < 0$ . We find that this phenomenology is maintained for  $l_t \in [0, -0.01]$ , before transitioning to a disordered gas for larger attractive translational interactions; this is shown in Figure 3(a). Putatively, the clumping tendency in this range is balanced by the excluded volume repulsions.

*Phenomenological non-linear hydrodynamics:* Our results can be rationalized via a phenomenological hydrodynamic (Toner-Tu-like [1]) description of our system, studying the linear stability of the flocking state to perturbations. We construct a minimal model for the density field  $\rho$  and the polarization field  $\mathbf{p}$  as follows:

$$\partial_t \rho = -\nabla \cdot [\rho u_0 \mathbf{p} - D_\rho \nabla \rho], \quad (4a)$$

$$\partial_t \mathbf{p} = (a_0 - a_1 |\mathbf{p}|^2) \mathbf{p} + a_2 \nabla^2 \mathbf{p} - \frac{u_1}{\rho_0} \nabla \rho, \quad (4b)$$

$$a_0 = (\beta_1 \chi_t - \chi_r) \left( v_s - \frac{\rho \chi_r}{c_1} \right), \quad a_1 > 0. \quad (4c)$$

Here  $\rho_0$  is the (spatial) average density,  $a_0$  and  $a_1$  are the decay and diffusion terms of the polarization field, whilst

$c_1$ , and  $\beta_1$  are free parameters of our model. The model is constructed such that  $a_0$  contains explicit dependencies on  $\chi_t$ ,  $\chi_r$ , whilst the other terms do not.  $u_0$  and  $u_1$  are the velocity and pressure terms respectively, whilst  $a_2$  and  $D_\rho$  are diffusion terms of the polarization and density fields respectively. A steady-state is  $\mathbf{p}$  obtained if

$$l_r < l_r^*, \quad l_r^* = \frac{c_1}{\rho} + \beta_1 l_t \quad (5)$$

We see that  $l_r^*$  also thus depends of the system density. An example of results from the simulation of (4) is shown in Fig. 3(b). We see that for parameters  $l_r > l_r^*$ , no global polar order is obtained, whereas for  $l_r < l_r^*$  the steady-state polarization of  $\sqrt{a_0/a_1}$  is obtained, corresponding to either the flock or band states seen in our particle-based simulations. The procedure for estimating the constants is as follows. First, the x-intercept from Fig. (2) is determined from which we get  $c_1 = 0.0104(8)$ . The slope of the transition line in Fig. (2) gives the  $\beta_1 \approx 6.01(4)$ . This fit line is shown on Fig. (2)(a) (dashed black).  $c_1$  then independently fixes the stability curve on Fig. 1(a); we see that the fit captures the transition fairly well. Further, we see that the details of the transition lines in the phase diagrams have an explicit dependence on  $[\rho, v_s]$ , also consistent with additional simulations we have performed (not here). In addition, we report that Eq. (5) also captures flock-to-disordered transition for attractive forces ( $\chi_t < 0$ ), see Fig. 3(a). Our model being minimal, it contains parameters  $a_1$ ,  $a_2$ ,  $D_\rho$ ,  $u_0$ , and  $u_1$  that are arbitrary. They could have explicit dependencies on microscopic  $\chi_t$ ,  $\chi_r$  or field  $\rho$  [12, 34], but that is not necessary to observe the transition we report. In addition, our model as it is does not capture the transition “from above” - for small  $\chi_r$  in Fig. 1(b)) and Fig. 2(a). Thus a more complete hydrodynamic description (via coarse-graining or otherwise) of the flocking phase of a fluid with internal torques and forces remain an open problem.

*Conclusions:* To conclude, we present a novel mechanism for flocking which only requires long-ranged (net) repulsive torques and short-ranged repulsive forces from hard-sphere interactions. Although the roles of excluded volume interactions [10, 11, 14, 16], repulsive torques - either short [10] or long [21] ranged - and long-ranged repulsive forces [16, 21] have been studied separately, we have analyzed here the individual contributions of each of those components, and argued that the former two are the minimal requisite component, whilst clarifying the mechanism for a fluidic flock formation via competing length (time) scales.

Our mechanism can summarized as follows: the chemotactic colloids slide together for a unit length before deterministically rotating away from each other. This is required to break the forward-backward symmetry at the pair-collision level. CLFs are indeed *both* generated by, and further destabilized by, the deterministic torques themselves. Another possible destabilization route is sufficiently high attractive forces. Both these routes render

the same effect in that a pair of colloids slide for too short or exceedingly long before rotating away upon collision. Notably, the apparent universal role of noise in destabilizing flocks [3, 7, 16, 21] is also absent in this mechanism (indeed we do not study it here). There is, thus, a narrow regime of deterministic rotational torques where a global polar order can emerge. We note that in the absence of short-ranged excluded volume repulsions, our model would converge to that recently studied in [21] where the need for (long-ranged) repulsive forces is more imminent. We also have not studied here the role of particle shape anisotropy [9, 12], which would add additional competing length scales to our analysis. Finally, the hydrodynamic

model presented here being minimal, we expect that a more rigorous derivation of similar equations to be forthcoming. These are thus left as potential future work.

We expect our results here to be directly relevant to a variety of experimental systems. For example, migrating cell collections have been widely reported to exhibit spatial organization resembling a polar fluid [17, 23], while their interaction mechanism has been known to include (among others) long-ranged chemotaxis and avoidance torques [22]. The presented mechanism being very generic, we expect it to also be relevant for interacting colloids of non-chemical origin [20, 32, 34], where the underlying mechanism should also hold.

- 
- [1] J. Toner, *The Physics of Flocking: Birth, Death, and Flight in Active Matter* (Cambridge University Press, 2024).
- [2] T. Vicsek, A. Czirók, E. Ben-Jacob, I. Cohen, and O. Shochet, Novel type of phase transition in a system of self-driven particles, *Physical review letters* **75**, 1226 (1995).
- [3] H. Chaté, F. Ginelli, G. Grégoire, and F. Raynaud, Collective motion of self-propelled particles interacting without cohesion, *Physical Review E—Statistical, Nonlinear, and Soft Matter Physics* **77**, 046113 (2008).
- [4] J. Toner, Y. Tu, and S. Ramaswamy, Hydrodynamics and phases of flocks, *Annals of Physics* **318**, 170 (2005).
- [5] J. Toner, Birth, death, and horizontal flight: Malthusian flocks with an easy plane in three dimensions, *Phys. Rev. E* **110**, 064604 (2024).
- [6] A. Maitra, P. Jentsch, L. Chen, C. F. Lee, J. Toner, and S. Ramaswamy, The inconvenient truth about flocks, *arXiv preprint arXiv:2503.17064* (2025).
- [7] S. Adhikary and S. Santra, Pattern formation and phase transition in the collective dynamics of a binary mixture of polar self-propelled particles, *Physical Review E* **105**, 064612 (2022).
- [8] S. Adhikary and S. Santra, Collective dynamics and phase transition of active matter in presence of orientation adapters, *arXiv preprint arXiv:2302.13035* (2023).
- [9] H. Wensink and H. Löwen, Emergent states in dense systems of active rods: from swarming to turbulence, *Journal of Physics: Condensed Matter* **24**, 464130 (2012).
- [10] M. Knežević, T. Welker, and H. Stark, Collective motion of active particles exhibiting non-reciprocal orientational interactions, *Scientific Reports* **12**, 19437 (2022).
- [11] L. Chen, K. J. Welch, P. Leishangthem, D. Ghosh, B. Zhang, T.-P. Sun, J. Klukas, Z. Tu, X. Cheng, and X. Xu, Molecular chaos in dense active systems, *arXiv preprint arXiv:2302.10525* (2023).
- [12] R. Großmann, I. S. Aranson, and F. Peruani, A particle-field approach bridges phase separation and collective motion in active matter, *Nature communications* **11**, 5365 (2020).
- [13] J. Chen, X. Lei, Y. Xiang, M. Duan, X. Peng, and H. Zhang, Emergent chirality and hyperuniformity in an active mixture with nonreciprocal interactions, *Physical Review Letters* **132**, 118301 (2024).
- [14] A. Martín-Gómez, D. Levis, A. Díaz-Guilera, and I. Pagonabarraga, Collective motion of active brownian particles with polar alignment, *Soft matter* **14**, 2610 (2018).
- [15] E. Sese-Sansa, I. Pagonabarraga, and D. Levis, Velocity alignment promotes motility-induced phase separation, *Europhysics Letters* **124**, 30004 (2018).
- [16] L. Caprini and H. Löwen, Flocking without alignment interactions in attractive active brownian particles, *Physical Review Letters* **130**, 148202 (2023).
- [17] T. Hiraiwa, Dynamic self-organization of idealized migrating cells by contact communication, *Physical Review Letters* **125**, 268104 (2020).
- [18] M. Kumar, A. Murali, A. G. Subramaniam, R. Singh, and S. Thutupalli, Emergent dynamics due to chemohydrodynamic self-interactions in active polymers, *Nature Commun.* **15**, 4903 (2024).
- [19] A. G. Subramaniam, M. Kumar, S. Thutupalli, and R. Singh, Rigid flocks, undulatory gaits, and chiral foldamers in a chemically active polymer, *New Journal of Physics* **26**, 083009 (2024).
- [20] A. Bricard, J.-B. Caussin, N. Desreumaux, O. Dauchot, and D. Bartolo, Emergence of macroscopic directed motion in populations of motile colloids, *Nature* **503**, 95 (2013).
- [21] S. Das, M. Ciarchi, Z. Zhou, J. Yan, J. Zhang, and R. Alert, Flocking by turning away, *Physical Review X* **14**, 031008 (2024).
- [22] B. A. Camley and W.-J. Rappel, Physical models of collective cell motility: from cell to tissue, *Journal of physics D: Applied physics* **50**, 113002 (2017).
- [23] M. Hayakawa, T. Hiraiwa, Y. Wada, H. Kuwayama, and T. Shibata, Polar pattern formation induced by contact following locomotion in a multicellular system, *Elife* **9**, e53609 (2020).
- [24] S. Saha, R. Golestanian, and S. Ramaswamy, Clusters, asters, and collective oscillations in chemotactic colloids, *Phys. Rev. E* **89**, 062316 (2014).
- [25] R. Soto and R. Golestanian, Self-assembly of active colloidal molecules with dynamic function, *Phys. Rev. E* **91**, 052304 (2015).
- [26] G. Rückner and R. Kapral, Chemically powered nanodimers, *Physical review letters* **98**, 150603 (2007).
- [27] R. Singh, R. Adhikari, and M. Cates, Competing chemical and hydrodynamic interactions in autophoretic colloidal suspensions, *The Journal of chemical physics* **151** (2019).

- [28] B. V. Hokmabad, J. Agudo-Canalejo, S. Saha, R. Golestanian, and C. C. Maass, Chemotactic self-caging in active emulsions, *Proc. Natl. Acad. Sci.* **119**, e2122269119 (2022).
- [29] B. Nijboer and F. De Wette, On the calculation of lattice sums, *Physica* **23**, 309 (1957).
- [30] Here  $\rho = N/L^2$ , where  $L$  is the length of the simulation box.
- [31] D. Geyer, A. Morin, and D. Bartolo, Sounds and hydrodynamics of polar active fluids, *Nature materials* **17**, 789 (2018).
- [32] D. Geyer, D. Martin, J. Tailleur, and D. Bartolo, Freezing a flock: Motility-induced phase separation in polar active liquids, *Physical Review X* **9**, 031043 (2019).
- [33] We note that our system is *effectively* noiseless; for values of  $D_t$  and  $D_r$  used here (see SI Section I), we have  $l_{\eta_t} = \frac{D_t}{v_s} \sim 10^{-8}$ , whilst  $l_{\eta_r} = \frac{D_r v_s b}{\chi_r} \sim 10^{-6}$ , whereas all other length scales are of  $O(10^{-2}) - O(1)$ .
- [34] J. Zhang, R. Alert, J. Yan, N. S. Wingreen, and S. Granick, Active phase separation by turning towards regions of higher density, *Nature Physics* **17**, 961 (2021).
- [35] R. A. Simha and S. Ramaswamy, Statistical hydrodynamics of ordered suspensions of self-propelled particles: waves, giant number fluctuations and instabilities, *Physica A: Statistical Mechanics and its Applications* **306**, 262 (2002).
- [36] J. Deseigne, S. Léonard, O. Dauchot, and H. Chaté, Vibrated polar disks: spontaneous motion, binary collisions, and collective dynamics, *Soft Matter* **8**, 5629 (2012).